

**CHAPTER VII**

**THERMO-ELECTRIC AND RESISTIVITY STUDIES OF**

**CERIUM AT HIGH PRESSURES**

CHAPTER VIITHERMO-ELECTRIC AND RESISTIVITY STUDIES OF CERIUM AT  
HIGH PRESSURES1. Introduction

Cerium, the rare-earth element after Lanthanum, exhibits remarkable high pressure behaviour and has been the subject of numerous experimental and theoretical investigations. The main interest in this substance is centered round the pressured-induced  $\gamma$ - $\alpha$  phase transition occurring near 7 kbar pressure at room temperature. It is interesting that among the elements, the phase diagram of cerium has many unique features such as a<sup>a</sup> solid-solid phase boundary ending up in a critical point and the melting curve exhibiting a minimum with respect to pressure. In recent years there has been a growing interest in the behaviour of  $\alpha$ -cerium which possesses such interesting features as the fractional valence, exchange enhanced susceptibility, etc.

It is now well understood that these interesting high pressure properties of cerium arises due to the proximity of a 4f virtual bound state to the Fermi level. The application of pressure essentially serves to vary the

relative separation between the localized 4f states and the Fermi level. The resonance scattering of conduction electrons by the 4f states lying close to the Fermi level is qualitatively different from say the 3d or 5d resonance. This is because the width of the 4f virtual bound state is extremely small compared with even the thermal spread near the Fermi level.

In this chapter we present new experimental results on the thermo-electric power and resistivity behaviour of cerium at high pressures. The reason for choosing thermo-power as a probe has been discussed in the previous chapter. The study of resistivity has been mostly confined to the region above the critical point where the  $\gamma$ - $\alpha$  phase transition is continuous. The experimental results reported in this chapter were obtained using the techniques described in the last chapter, viz., the teflon-cell technique, the High temperature High pressure thermo-power cell and the automatic recording system. Thermo-power has been measured in the temperature range 10°-400°C and up to 30 kbar pressure. The temperature variation of the resistivity in the  $\gamma$  and  $\alpha$  phases is also reported. The new measurements on the resistivity include the study of resistance versus pressure isotherm at 275°C.

The important results that have emerged out of the study of the thermo-power variation with pressure are briefly summarized.

(i) The absolute thermo-power of cerium varies markedly with pressure in the  $\gamma$ -phase region which is in sharp contrast with the resistivity behaviour in the same region.

(ii) The  $\gamma$ - $\alpha$  phase transition manifests itself as a sharp decrease in the magnitude of the thermo-electric power.

(iii) At room temperature, the thermo-power of  $\alpha$ -cerium decreases continuously with pressure leading to a change of sign at higher pressures.

(iv) The temperature variation of the thermo-power shows a remarkable behaviour in the  $\alpha$ -phase. In the low pressure region of the  $\alpha$ -phase, the thermo-power rises sharply from negative values to large positive values, over a narrow temperature range. Further this rate of increase of thermo-power with temperature decreases with increase of pressure in the  $\alpha$ -phase region.

The main result of our resistivity studies on cerium is concerned with its behaviour above the critical point. The resistivity versus pressure isotherm exhibits

a broad maximum as the virtual bound state moves continuously from below to above the Fermi level. This verifies the earlier prediction of Blandin et al (1965) regarding the resistivity behaviour above the critical point.

An attempt has been made to explain these experimental results on the basis of the Friedel-Anderson model (Friedel, 1956; Anderson, 1961) and Hirst's development of this model (Hirst, 1970). The thermo-power variation in the  $\gamma$ -phase with pressure can be qualitatively explained on the basis of the virtual bound state description appropriate to cerium. The continuous decrease in the thermo-power with pressure and its anomalous temperature behaviour in the  $\alpha$ -phase can be correlated with the fractional valence model of  $\alpha$ -cerium. The resistivity behaviour also finds a simple explanation.

## 2. Experimental Situation - A Brief Survey

Bridgman (1927, 1951) first reported the resistance discontinuity indicative of phase transformation in cerium near 7 kbar pressure at room temperature. Later Lawson and Tang (1949) from their high pressure X-ray diffraction work established that this phase transformation involves only a decrease in the lattice parameter without any change

in symmetry. At room temperature and atmospheric pressure, cerium has the face centered cubic structure ( $\gamma$ -phase) with a lattice parameter of  $5.16 \text{ \AA}$  and is paramagnetic. After the phase transformation, the structure is still f.c.c. ( $\alpha$ -phase) but with a decreased lattice parameter of  $4.85 \text{ \AA}$ . Further the  $\alpha$ -phase is non-magnetic. Schuch and Sturdivant (1950) observed the same transformation at atmospheric pressure when  $\gamma$ -cerium is cooled below  $100^\circ\text{K}$ . Zachariasen (quoted by Lawson and Tang, 1949) and independently Pauling (quoted by Schuch and Sturdivant, 1950) suggested that the iso-structural  $\gamma$ - $\alpha$  transition involves the 4f-5d electron promotion. The delocalization of 4f electrons destroys the magnetic moment of the ion cores in the  $\alpha$ -phase and this has been confirmed from the neutron diffraction studies of Wilkinson et al (1961). Hall effect measurements on the  $\gamma$  and  $\alpha$  phases (Gschneidner and Smoluchowski, 1963) support the view that there is a definite change in the valency accompanying the transition. The valences of  $\gamma$  and  $\alpha$ -Ce have been estimated (Gschneidner, 1964) from Hall effect studies to be 3.06 and 3.67 respectively.

Beecroft and Swenson (1960) from their measurements of the lattice parameter decrease at different temperatures made the remarkable prediction that the

discontinuous volume change in the  $\gamma$ - $\alpha$  transition should disappear near 20 kbar pressure and 630°K. Penyatovskii (1958) found that at  $P = 18$  kbar and  $T = 553^\circ\text{K}$ , the heat of transition vanished. Jayaraman (1965) from his studies on the resistivity variation with pressure at various temperatures established that a critical point exists for the  $\gamma$ - $\alpha$  transition at about 550°K and 17.5 kbar pressure.

The phase diagram of cerium is presented in Figure 1. The boundary between  $\gamma$  to  $\alpha$ -Ce was delineated by Jayaraman (1965) using the resistance discontinuity method. Figure 2 presents the resistance versus pressure isotherms for cerium taken from the work of Jayaraman (1965). These curves indicate that the magnitude of the resistance drop progressively diminish with temperature. The isotherm for 598°K does not show any discontinuous resistance drop, and the resistance of the sample varies smoothly with pressure.

The main features of the phase diagram (Figure 1) can be briefly summarized as follows. Among the elements the phase diagram of cerium is perhaps unique in that a solid-solid phase boundary terminates at a critical point. It is to be noted that a critical point can exist only for phases between which the difference is of a purely quantitative nature and which do not differ in internal

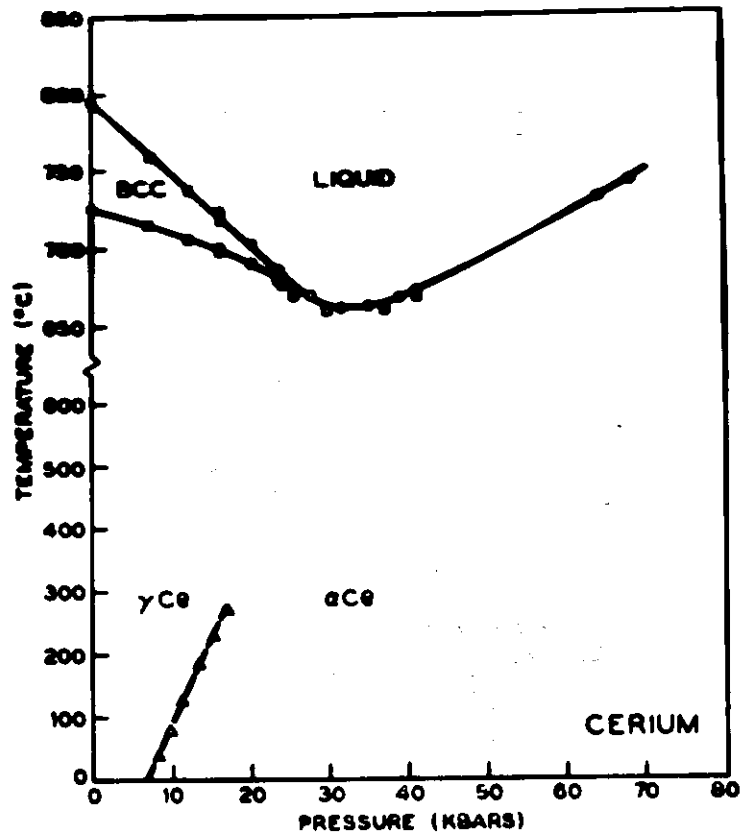


Fig. 1. Phase diagram of cerium

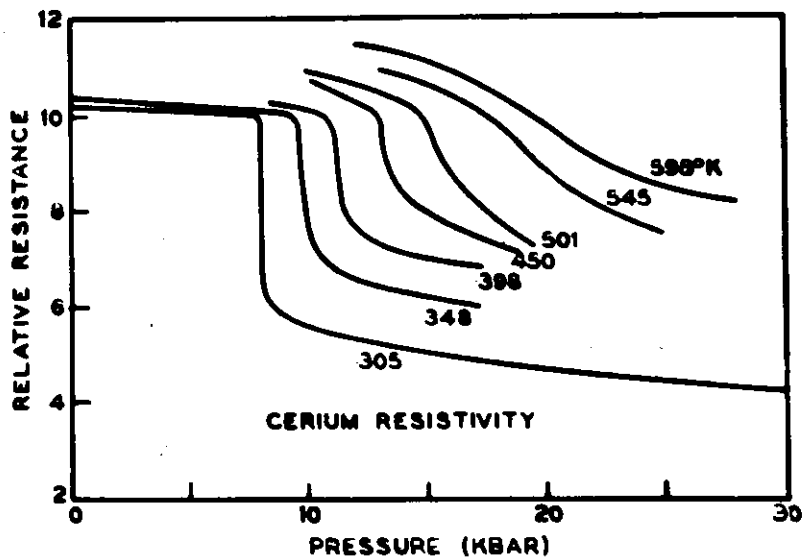


Fig. 2. Pressure-resistance isotherms of fcc-cerium

symmetry (Landau and Lifshitz, 1958). Above the critical point, the  $\gamma$ - $\alpha$  phase transition is continuous involving a progressive diminution in the atomic volume. According to Blandin et al (1965) there should exist another line in the phase diagram above the critical point representing a second order transition from the non-magnetic ( $\alpha$ -phase) to the magnetic cerium metal ( $\gamma$ -phase).

The fusion curve minimum in cerium near 30 kbar pressure is another interesting feature of the phase diagram. It may be noted that the  $\gamma$  to  $\alpha$ -Ce boundary when extrapolated intersects the melting curve at the minimum. The application of the Clausius-Clapyeron equation to the fusion curve minimum indicates a rapid increase in the density of the neighbouring solid. The region of f.c.c.-Ce bordering the liquid lies in the phase diagram above the critical point for the  $\gamma$ - $\alpha$  transition. In the region lying close to the extrapolated  $\gamma$  to  $\alpha$ -Ce phase boundary, there will be a rapid variation in the density with pressure due to the continuous phase transformation. Thus the fusion curve minimum really corresponds to the supercritical behaviour of f.c.c. cerium.

#### Magnetic Studies on Cerium at High Pressures:

The  $\gamma$ - $\alpha$  transition corresponding to the magnetic f.c.c. to the non-magnetic f.c.c. structure can be probed

using magnetic susceptibility measurements as a tool. Experimentally the measurements of the paramagnetic susceptibility at high pressures is difficult due to the large diamagnetic contribution of the specimen and the specimen holder. However, using special techniques (Wohlleben, 1968), MacPherson et al (1971) have made measurements of the magnetic susceptibility of cerium at high pressures. These experiments have thrown more light on the unusual properties of the  $\alpha$ -phase and we briefly summarize the experimental results. The  $\gamma$ -phase which is characterized by a localized moment exhibits the well-known Curie behaviour with temperature. The magnetic susceptibility of  $\gamma$ -Ce decreases with pressure in the pre-transition region and the  $\gamma$ - $\alpha$  transformation manifests as a drastic drop in the magnitude of the susceptibility. The effect of pressure is again considerable in the  $\alpha$ -phase and the susceptibility decreases by nearly 20% between 8 and 18 kbar, linearly with pressure. The magnetic susceptibility is nearly temperature independent in the  $\alpha$ -phase suggesting that  $\alpha$ -Ce is basically a Pauli paramagnet, i.e., there is no localized magnetic moment in the  $\alpha$ -phase. However in the  $\alpha$ -phase there is a strong local exchange enhancement of the susceptibility. Using the available electronic specific heat data, Macpherson et al (1971) found for the un-renormalized exchange enhancement,

a value of the order of 8. This exchange enhancement and the molar susceptibility itself are very large and are only comparable with Palladium in the periodic table. This is compatible with the absence of superconductivity in the  $\alpha$  phase (Smith, 1965). However superconductivity has been observed (Wittig, 1968) in a high pressure phase at pressures higher than 50 kbar. The structure of the superconducting high pressure phase known as the  $\alpha'$ -phase is still not well established. Franceschi and Olcese (1969) reported that the structure of  $\alpha'$ -phase is again f.c.c., with a lattice parameter of 4.66 Å. However McWhan (1970) found that the  $\alpha'$ -phase is not f.c.c., but a distorted h.c.p. structure. Setting apart the controversy on the structure of  $\alpha'$ -phase, one could still deduce that near 50 kbar pressure, cerium behaves a truly four valent metal and that the 4f level is sufficiently far from the Fermi level. Ratto et al (1969) have considered theoretically, the influence of the 4f character on the existence of superconductivity and conclude that a strong 4f character (which inhibits superconductivity) persists in the low pressure region of the  $\alpha$ -phase.

### 3. Theoretical Situation - A Brief Survey

#### 3.1. Friedel-Anderson Model:

The concept of a 'virtual bound state' (Friedel, 1954), apart from explaining the anomalous electronic

properties of alloys, has played a significant role in our understanding of the origin of the 'localized moments' in some metals. It is well-known that in a variety of cases of 3d transition metal impurities in simple metals, the magnetic susceptibility exhibits a Curie-like behaviour. This implies that the impurities possess localized magnetic moments and the basic question regarding the conditions under which such a magnetic state is formed was first considered in a classic paper by Friedel (1956). In terms of the virtual bound state description of the energy level of an impurity atom which lies in the conduction band of the matrix, the question of the existence of a magnetic moment reduces to one of finding the conditions under which the virtual states for spin  $\sigma$  are not equivalent with those of spin  $-\sigma$ . The basic interaction responsible for breaking the symmetry of the virtual bound state with respect to spin polarization has been postulated to be the local particle-particle coulomb repulsion  $U$  between electrons of opposite spin when on the impurity site. Basically, this is the same interaction that makes the moments align parallel in an isolated atom in accordance with Hund's rule. However, the magnitudes of the parameters like the coulomb repulsion energy  $U$ , the width of resonance  $\Delta$  and the position of the resonance energies for up and down spin polarizations in relation to the Fermi level, are the

deciding factors regarding the localized moment formation. Physically, the formation of the moment can be visualised as follows. Let the resonance energy  $E_d$  corresponding to up or down spin polarization be sufficiently below the Fermi level  $E_F$ . It is then clear that the coulomb interaction shifts the resonance energy of opposite spin to  $E_d + U$ . If  $E_d + U$  is located above the Fermi level, then the second electron falls into the Fermi sea leading to moment formation. On the other hand, if  $E_d + U$  is also located below the Fermi level then both the electrons of opposite spins will occupy the impurity level resulting in the loss of moment. Anderson (1961) in his classic paper has discussed the problem of localized magnetic states in detail and also gave the conditions for the realization of a magnetic state. The results of the Anderson model can also be derived from scattering formalism. The development of the Friedel-Anderson model for localized moments and its relation to the Kondo effect have been excellently reviewed by Heeger (1969) and Kondo (1969).

The Friedel-Anderson model, although originally developed to deal with the dilute magnetic impurities in alloys, can also be applied to the localized 4f states in cerium. Blandin et al (1965) and Coqblin and Blandin (1968) have provided the justification for this by noting that the

spatial extent of the 4f shell is much smaller than the lattice constant of cerium. The direct overlap of 4f electrons on neighbouring atoms is extremely small. The admixture of the conduction and localized states leads to a width of the virtual bound state of the order of  $10^{-2}$  eV. Thus the 4f states in cerium represent typically the case of an impurity.

### 3.2. Blandin, Coqblin and Friedel's Model for Cerium:

Blandin et al (1965), in their well-known paper, considered the stability of the magnetic moments under pressure in rare earth metals. Their theory based on the Friedel-Anderson model could account for the main features of the  $\gamma$ - $\alpha$  phase transition. This first order phase transition is characterized by an abrupt variation in the magnetic moment and in the number of localized electrons. The driving force responsible for the phase transition in this model is provided by the so called compression-shift mechanism. The effect of pressure is to increase the value of the Fermi energy relative to the bottom of the conduction band. However the energy of the bottom of the conduction band decreases more rapidly with pressure so that the absolute value of the Fermi energy decreases. The energy of the 4f states remains nearly the same with pressure. Thus the energy gap

between the localized 4f states and the Fermi energy decreases under pressure. At a critical value of the energy of 4f state there is a drop in the number of localized electrons corresponding to the  $\gamma$ - $\alpha$  first order transition. Blandin et al (1965) also noted that the effect of temperature would be quite considerable when  $kT$  is of the order of the energy gap between the 4f state and the Fermi level. These authors have predicted that above the critical point, the phase transition is one of second order characterized by a continuous appearance of a magnetic moment. Experimental confirmation of this interesting prediction of a tricritical point would throw more light on the nature of the phase transition at higher temperatures. Another prediction of the theory is regarding the resistivity behaviour above  $T_c$ . As the virtual bound state moves continuously under pressure from below to above the Fermi level, one should expect a large maximum in the resistivity versus pressure graph. The effect of temperature, as the authors have pointed out, is however to reduce this maximum.

### 3.3. Ramirez-Falicov Model:

Ramirez and Falicov (1971) have proposed an alternative mechanism for the  $\gamma$ - $\alpha$  phase transition. In this model the driving force for the transition is assumed to be

the Coulomb repulsion between the localized 4f electrons and the conduction electrons derived from the 6s-5d band. Recently Alascio et al (1973) have extended the Ramirez-Falicov theory to include the effects associated with the hybridization of the 4f states with the conduction band. These authors have also derived the magnitudes of the electronic specific heat, magnetic susceptibility and fractional valency of the  $\alpha$  phase.

#### 3.4. Hirst's model:

Hirst (1970) has modified the Friedel-Anderson model with particular emphasis on the nature of the inter-configurational cross-over from  $4f^1$  to  $4f^0$  occurring in cerium. He has criticized the Ramirez-Falicov theory on the ground that the dependence of the electronic energies is parametrized as a function of pressure instead of volume. This is unsatisfactory in view of the fact that the phase transition is characterized by a discontinuous pressure-volume relation. Hirst's theory focusses attention on the question of whether the cross-over phenomenon occurs discontinuously and whether a fractional-valence thermodynamic state, in which the individual 4f ions undergo rapid inter-configurational fluctuations, is stable near the cross-over. The configurational cross-over phenomenon corresponds to the 4f virtual bound state going from below to above the

Fermi level. If  $E_{\text{exc}}^{(-)}$  is defined as the energy necessary to make an inter-configuration excitation from  $4f^1$  to  $4f^0$ , then in the cross-over process  $E_{\text{exc}}^{(-)}$  goes from positive to negative values. In the Hirst's theory,  $E_{\text{exc}}^{(-)}$  behaves anomalously at the cross-over, tending either to jump discontinuously, or on the contrary to 'lock' to the value zero. In the latter case  $E_{\text{exc}}^{(-)}$  remains zero as the pressure is varied and the corresponding thermodynamic state has remarkable properties. When  $E_{\text{exc}}^{(-)}$  is extremely small, the individual ions undergo spontaneous inter-configuration fluctuations by emission and absorption of conduction electrons, with a fluctuation rate of order  $\Delta/\hbar$  where  $\Delta$  is the width of the  $4f$  virtual bound state. Thus for time scales shorter than  $\hbar/\Delta$ , the ions are in a well defined configuration whereas for times longer than  $\hbar/\Delta$  the ions are characterized by a statistical average of the two configurations. In Hirst's model this is the origin of the intermediate or fractional valence observed in the  $\alpha$  phase of cerium. Further while considering the magnetic moment of the ion, it becomes relevant to specify the time interval as compared to the characteristic time  $\hbar/\Delta$ . Maple and Wohlleben (1971) have provided an explanation for the magnetic behaviour of  $\alpha$ -Ce and the high pressure phase of Samarium Sulphide on the basis of the Hirst's model.

#### 4. Thermo-Power Study of Cerium with Pressure

##### 4.1. Experimental Results Using Teflon-Cell Technique:

The thermo-power variation up to 30 kbar pressure and in the temperature range 10-100°C was studied using the teflon-cell technique described in Section 4 of Chapter VI. The cell design presented there needs only a slight modification for a solid specimen. Figure 3 presents the teflon-thermo-power cell appropriate to solid specimens. The specimen cut in bar form was pierced into the centre of a teflon disc and this assembly is then inserted into a teflon container filled with silicone liquid. The rest of the arrangement remains the same.

The cerium metal used in these studies was of high purity obtained from Research Chemicals, Inc. (U.S.A). The structure of a well-annealed sample at room temperature and atmospheric pressure is f.c.c. ( $\gamma$ -phase) and it is known that cold-working results in a mixture of the  $\gamma$ -phase and the  $\beta$ -phase, which has a double hexagonal close-packed structure. Since we are mainly interested in the  $\gamma$ -phase, the structure of the starting material was checked. X-ray diffractometer record confirmed that the starting material was completely  $\gamma$ -phase.

Figure 4 presents the thermo-power variation with temperature up to 100°C at different pressures. The data

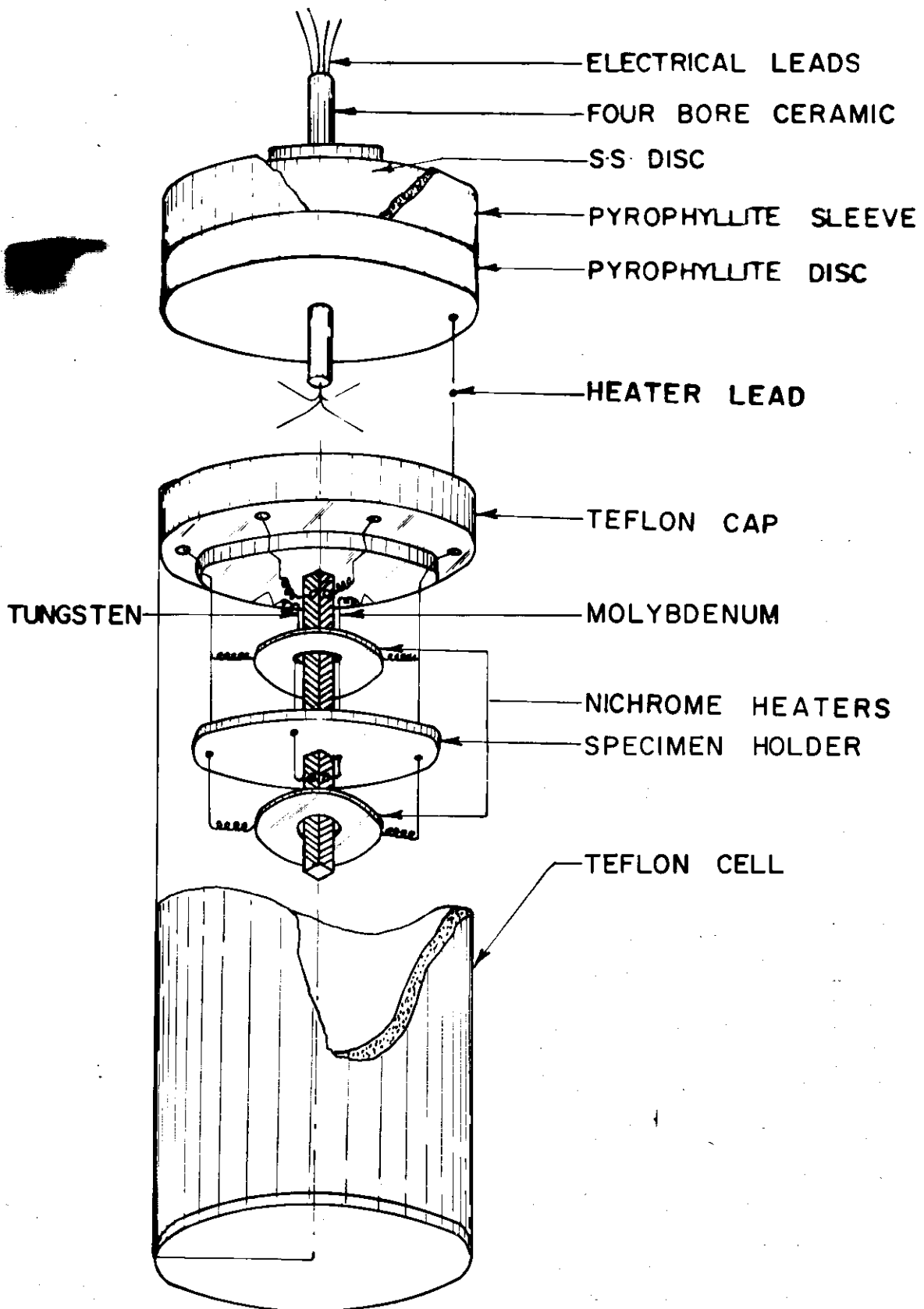


Fig. 3. Thermo-power cell for a solid specimen.

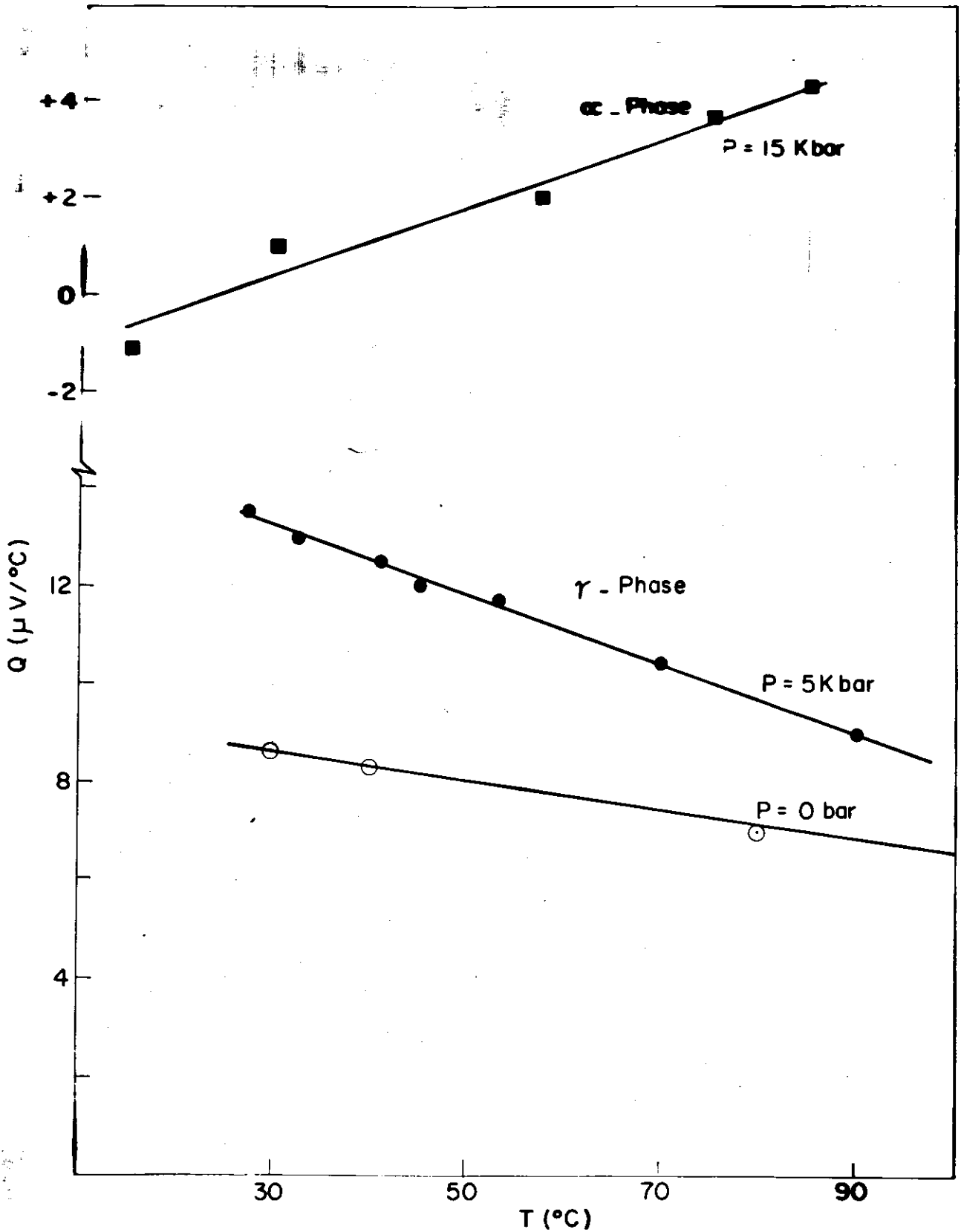


Fig. 4. Variation of the thermo-power of cerium with temperature in the  $\gamma$  and  $\alpha$  phases.

points on these graphs were obtained using two different thermocouple probes, viz., chromel-alumel and molybdenum-tungsten wires. The experimental results in the  $\alpha$ -phase region and at higher pressures were derived mostly using the Mo-W thermocouple. This was necessitated by the much smaller magnitude of  $Q_{ce}$  ( $\approx 0.5 \mu\text{V}/^\circ\text{C}$ ) as compared with either  $Q_{\text{chromel}}$  ( $\approx +22 \mu\text{V}/^\circ\text{C}$ ) or  $Q_{\text{alumel}}$  ( $\approx -18 \mu\text{V}/^\circ\text{C}$ ). In the  $\gamma$ -phase region,  $(\frac{dQ}{dT})$  is negative. It is interesting that in the  $\alpha$ -phase  $(\frac{dQ}{dT})$  changes sign. Further  $Q_{ce}$  also changes sign in the  $\alpha$ -phase from positive to negative values at lower temperatures.

Figure 5 shows the behaviour of the thermo-electric power of cerium as a function of pressure at constant mean temperature of  $30^\circ\text{C}$ . The salient features of this isotherm are summarized below.

a) In the  $\gamma$ -phase region, the pressure variation of the thermo-electric power is rather large leading to a cusp like behaviour prior to the phase transition. This remarkable variation in the thermo-power from nearly  $7 \mu\text{V}/^\circ\text{C}$  at atmospheric pressure to about  $20 \mu\text{V}/^\circ\text{C}$  near the phase transition is in sharp contrast to the resistivity behaviour in the same region. The experimental data of Jayaraman(1965)

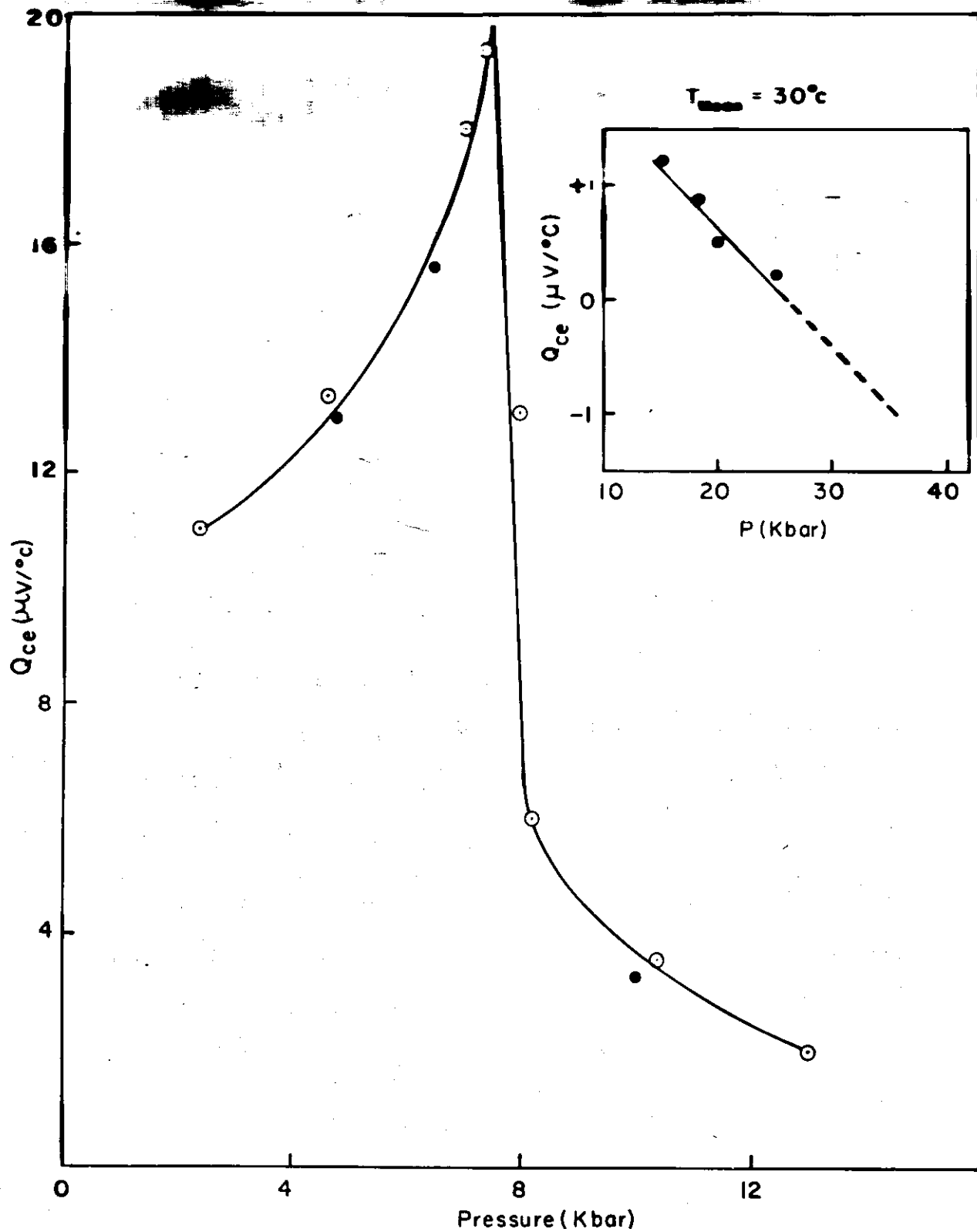


Fig. 5. Thermo-electric power versus pressure graph for Cerium at 30°C.

● - Data points obtained using Mo-W thermocouple.

⊙ - Data points obtained using Chromel Alumel thermocouple.

on resistivity behaviour (Figure 2) indicates only a slight decrease of resistivity in this pressure region.

b) The first order  $\gamma$ - $\alpha$  phase transition associated with the delocalization of the 4f electrons manifests as a sudden drop in the magnitude of the thermo-power from nearly  $20 \mu\text{V}/^\circ\text{C}$  to  $5 \mu\text{V}/^\circ\text{C}$ .

c) In the  $\alpha$ -phase region, there is a continuous decrease in the magnitude of thermo-power with pressure. The pressure coefficient of thermo-power in  $\alpha$ -phase region is quite considerable of the order of  $-0.27 \mu\text{V}/^\circ\text{C kbar}$ . Further the sign of the thermo-power changes at higher pressures. The inset in Figure 5 suggests that near 40 kbar pressure, the value of  $Q_{ce}$  would be of the order of  $-1 \mu\text{V}/^\circ\text{C}$  at room temperature.

The temperature behaviour of the thermo-power in the  $\alpha$ -phase over a small temperature range of  $15$ - $40^\circ\text{C}$  is given in Figure 6. The general feature of all the curves, viz., at 16.5 kbar, 23 kbar and 18.7 kbar is the strong upward curvature at lower temperatures. The nature of these graphs indicate that the thermo-power would be strongly negative in the temperature region lower than  $0^\circ\text{C}$ . From Figures 6 and 5 one could deduce that the isotherms at lower temperatures ( $<0^\circ\text{C}$ ) of the thermo-power versus pressure graph would exhibit a greater anomaly. The  $\gamma$ - $\alpha$  transition

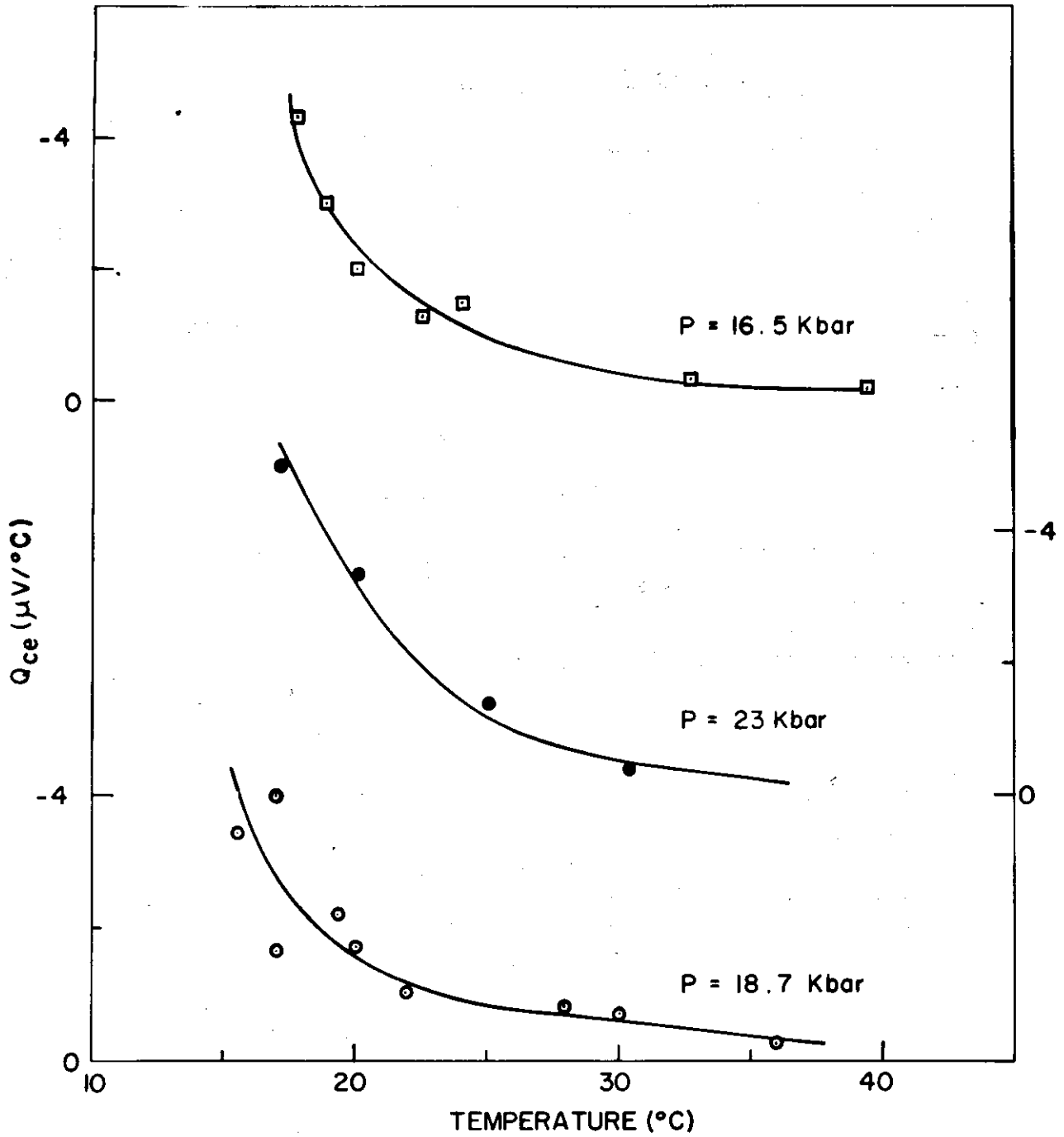


FIG. 6 THERMO-POWER Vs TEMPERATURE GRAPH FOR CERIUM IN THE  $\alpha$ - PHASE (TEFLON CELL TECHNIQUE)

at low temperatures may be expected to manifest itself as a change of sign from large positive values to negative values.

#### 4.2. Experimental Results Using High Temperature-High Pressure Thermo-Power Cell:

The limitation of the teflon cell technique for thermo-power measurement is that the maximum temperature of measurement is around 200°C. Our interest in studying the thermo-power and resistivity around the critical point, characterized by a nearly 300°C and 18 kbar pressure, led us to the development of the high temperature and high pressure thermo-power cell. This has been described in section 5 of chapter VI. We present here the experimental results on thermo-power obtained using this cell arrangement.

Figure 7 presents the thermo-power versus temperature graph in the temperature region 50°-350°C at two pressures, viz., P=4 kbar and P=9.6 kbar. Both the curves correspond to the behaviour in the  $\gamma$ -phase. It may be noted that the curve for P=9.6 kbar has a considerable non-linear behaviour with temperature.

Figure 8 presents a series of thermo-power versus temperature curves at different pressures covering the region of both below and above the critical point in the phase diagram (Figure 1). These curves represent the  $\gamma$ - $\alpha$  phase

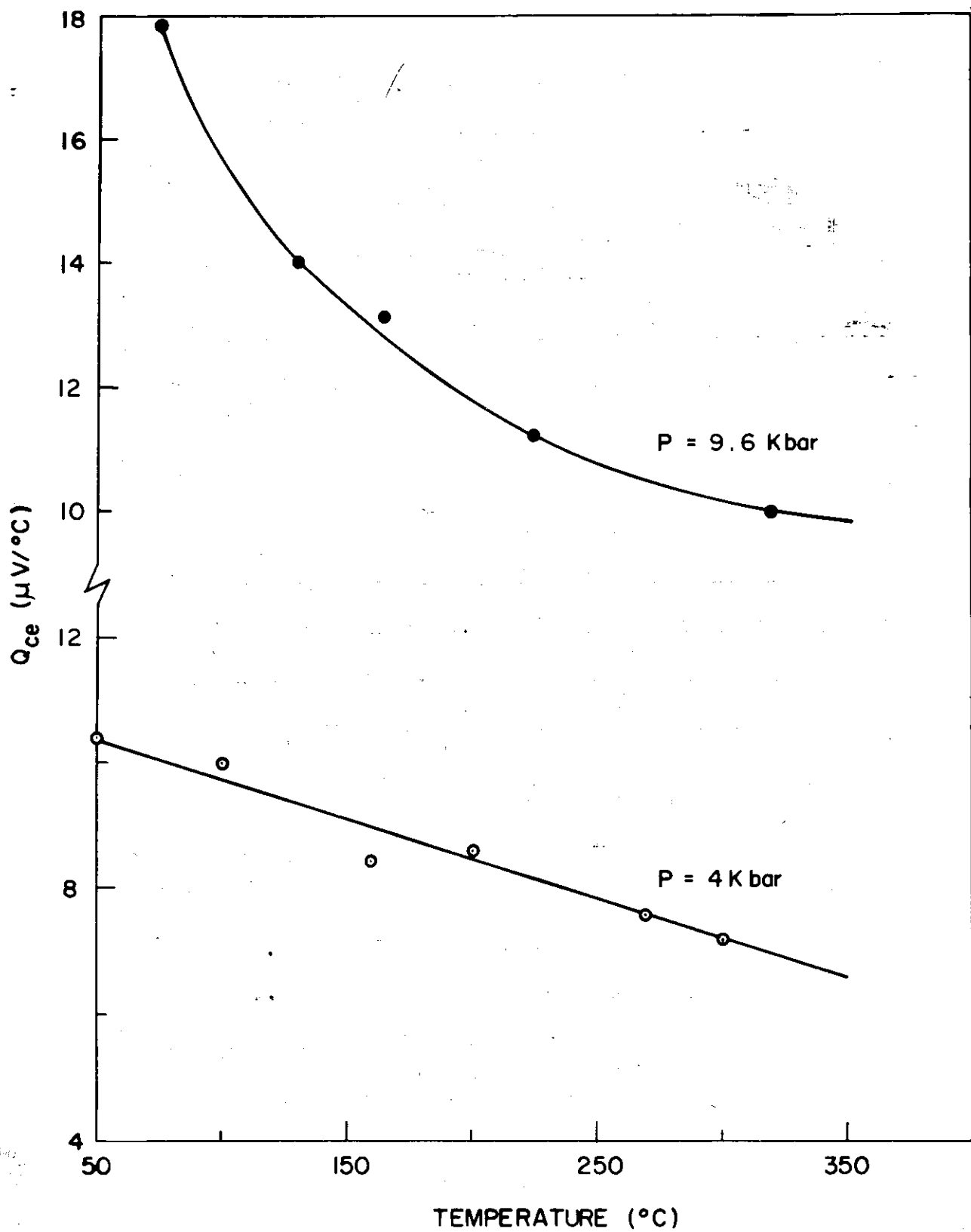


FIG. 7 THERMO-POWER VS TEMPERATURE GRAPH IN THE HIGH TEMPERATURE REGION.

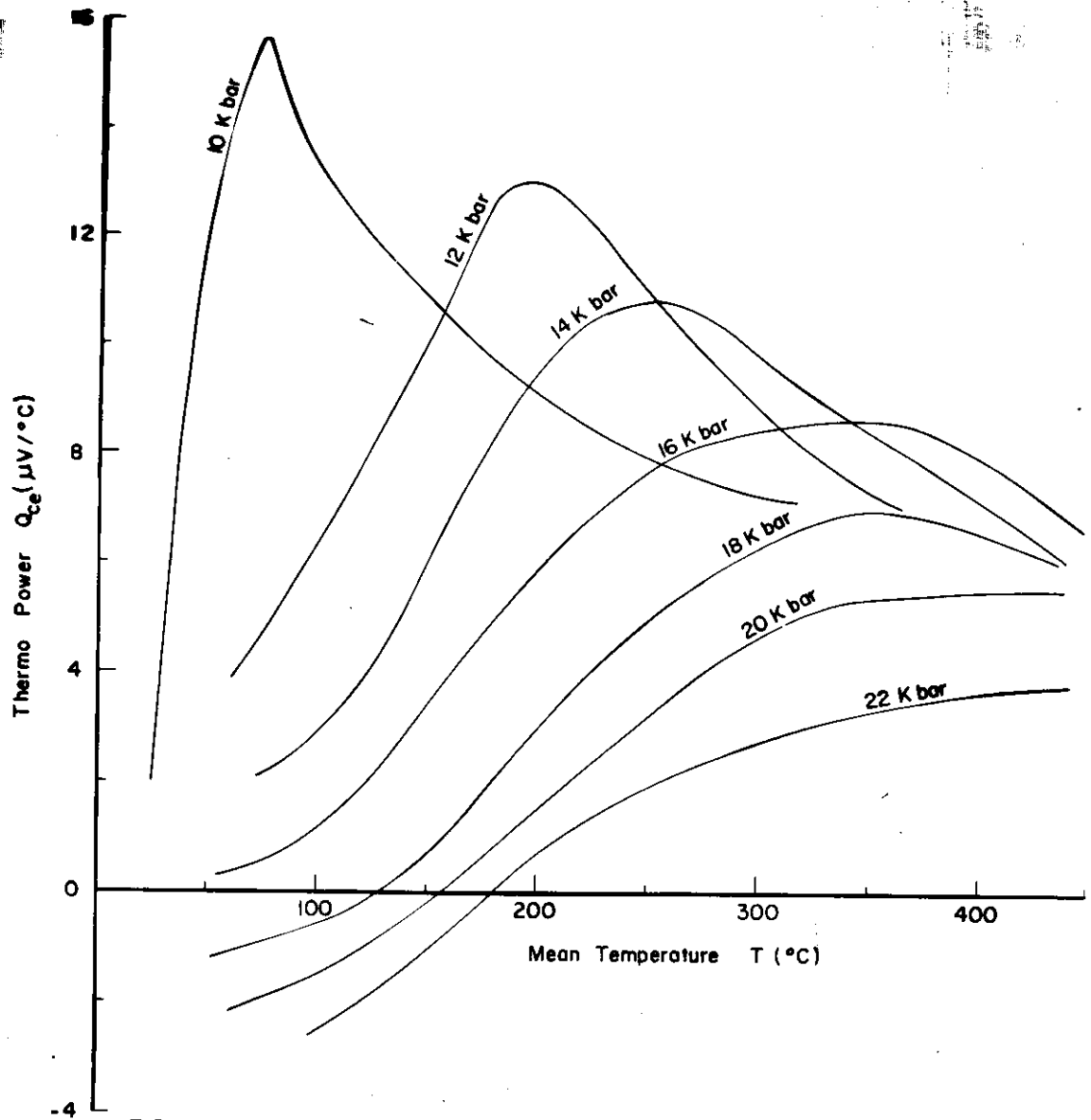


FIG. 8. VARIATION OF  $Q$  AS A FN. OF MEAN TEMP.  $T$  AT DIFFERENT PRESSURES.

transition studied through thermo-power variation with temperature keeping the pressure constant, corresponding to crossing the phase boundary vertically in the phase diagram (Figure 1). The pressure values marked in these diagrams are accurate to only  $\pm 1$  kbar. This is because of the use of a solid pressure communicating medium in the cell arrangement. Although silver chloride is known to be <sup>the</sup> best available solid pressure transmitting medium, its reactivity with metals makes it unsuitable for these studies. We have used Boron nitride, which is <sup>the</sup> next best for the pressure communicating medium. While interpreting these experimental results, it must be borne in mind that the specimen is not subjected to a truly hydrostatic pressure.

It was noted earlier that the temperature coefficient of thermo-power in the  $\gamma$ -phase is negative whereas in  $\alpha$ -phase it is positive. Thus the initial rise of thermo-power with temperature in all the curves corresponds to its behaviour in the  $\alpha$ -phase and the subsequent drop with temperature signifies the  $\alpha$ - $\gamma$  phase transition at constant pressure. The position of maximum shifts to higher temperatures as the pressure is increased in accordance with the phase diagram. From the diagram it is clear that the 16 kbar and 18 kbar isobars show a tendency for flattening and one could deduce that these curves and the higher pressure isobars correspond

to the behaviour above the critical point. The pressure and temperature co-ordinates of the critical point is approximately 18 kbar and 325°C.

The most interesting feature of these isobaric curves is the dramatic increase in the thermo-power with temperature in the  $\alpha$ -phase. The isobar corresponding to 10 kbar pressure, in particular, shows that over a small temperature range of 25°-50°C, the thermo-power increases from nearly 2  $\mu\text{V}/^\circ\text{C}$  to 10  $\mu\text{V}/^\circ\text{C}$ . That is  $\frac{dQ}{dT}$  at 10 kbar is approximately +0.35  $\mu\text{V}/^\circ\text{C}^2$ . One can expect that the isobars corresponding to pressures lesser than 10 kbar and transition temperatures lower than 0°C will be characterized by a much more steeper increase of thermo-power with temperature. The rate of increase of thermo-power with temperature decreases with increase of pressure. The magnitude of  $\frac{dQ}{dT}$  at 20 kbar pressure is approximately +.03  $\mu\text{V}/^\circ\text{C}^2$ , which is nearly ten times smaller than the corresponding quantity for 10 kbar pressure.

Figure 9 presents the thermo-power versus pressure isotherms constructed out of the data in Figures 8 and 7. It can be seen from the diagram that the magnitude of the anomaly decreases as the temperature is raised, which is quite similar to the resistivity behaviour (Figure 2). The sharpness in the discontinuity can be used as a criterion

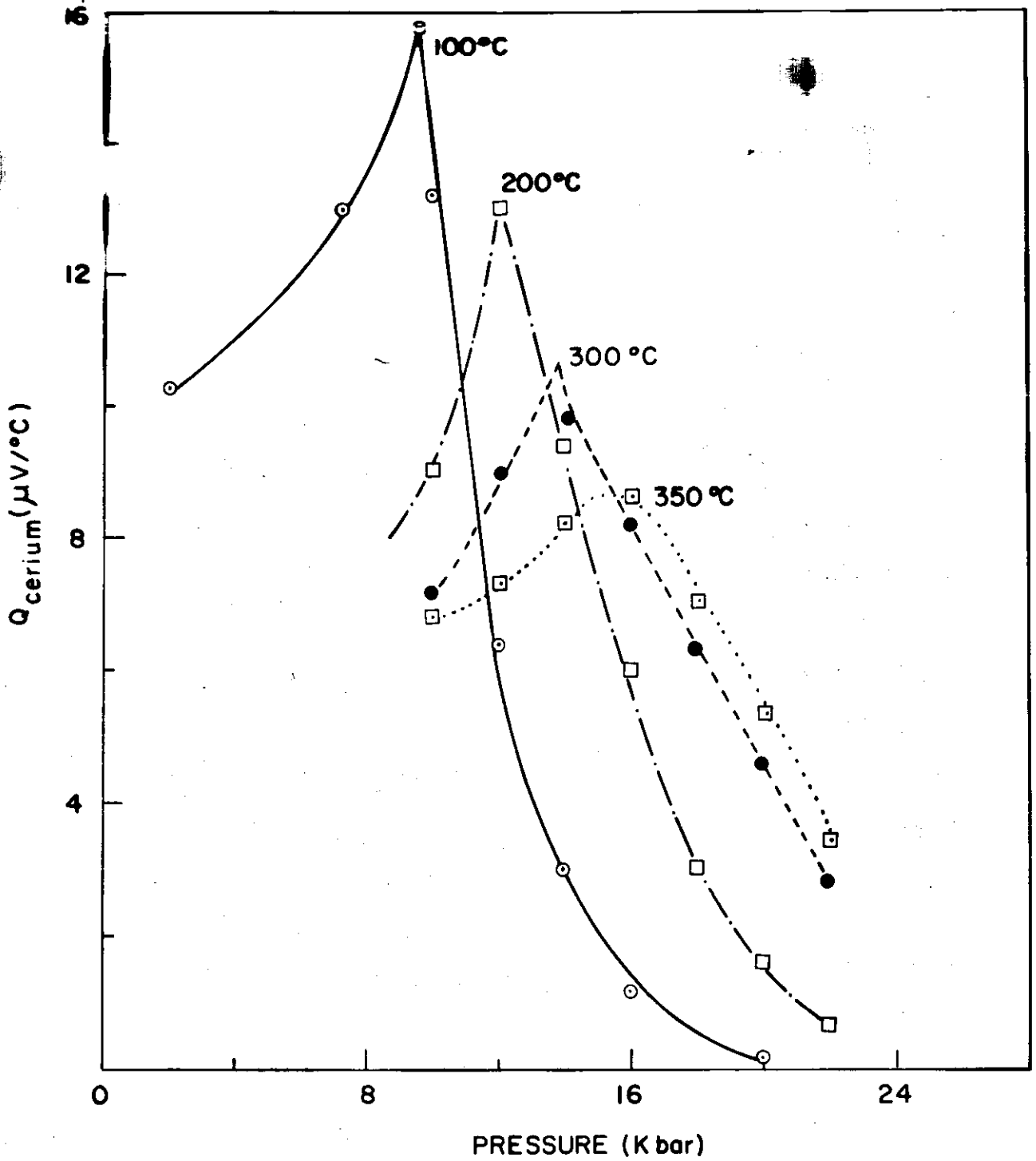


FIG. 9 ISOTHERMS OF THE THERMO-POWER Vs PRESSURE DATA FOR CERIUM.

for distinguishing whether the phase transition is first order or continuous. Strictly speaking the isotherms at 100°C and 200°C should exhibit a near vertical drop at pressures appropriate to the  $\gamma$ - $\alpha$  phase transition. The width of the experimental curves for 100°C and 200°C which is around two kbars on the pressure scale is an artifact of the experimental set up, viz., the use of a solid pressure transmitting medium which does not impart a truly hydrostatic pressure over the sample. This can be seen more clearly by comparing the isotherm at 30°C (Figure 5) obtained using the teflon-cell with those corresponding to 100°C and 200°C. However the isotherms corresponding to 300°C and 350°C have much larger widths than the experimental width and this is attributed to the continuous phase transformation above the critical point.

##### 5. Experimental Results of the Resistivity of Cerium at High Pressures

The experimental work of Jayaraman (1965) on the resistivity behaviour was mainly directed towards establishing the critical point and also to delineate the  $\gamma$ - $\alpha$  phase boundary. We present here our experimental results on the temperature behaviour of the resistivity in the  $\gamma$  and  $\alpha$  phases and new data on the resistivity versus pressure isotherm above the critical point.

Figure 10 presents the relative resistance versus pressure graph for two pressures, viz.,  $P = 0.8$  kbar and  $P = 12.6$  kbar. These data were obtained using the teflon-cell technique and internal heating arrangement described by Maines (1970). A.C. resistance measurement with the four probe method was resorted to, for this eliminates the thermo e.m.f.'s in the circuit which invariably arise in a d.c. type of measurement. The main feature of the experimental curves is that temperature affects markedly the resistivity of  $\alpha$ -Ce whereas its effect is negligible in the  $\gamma$ -phase. In fact the temperature coefficient of resistance in the  $\alpha$ -phase is nearly three times larger than the corresponding quantity in the  $\gamma$ -phase.

Figure 11 shows the relative resistance versus pressure isotherm just above the critical point. This data was collected using the High temperature High pressure cell described in the previous chapter. The two pairs of thermocouple probes served as current and voltage leads. The relative resistance could be directly plotted as a function of pressure by slow compression.

The salient features of this curve are that

(i) the resistivity decreases initially with pressure leading to a shallow minimum around 12 kbar, (ii) there is a rapid increase in the resistivity between 12 to 17 kbar pressure,

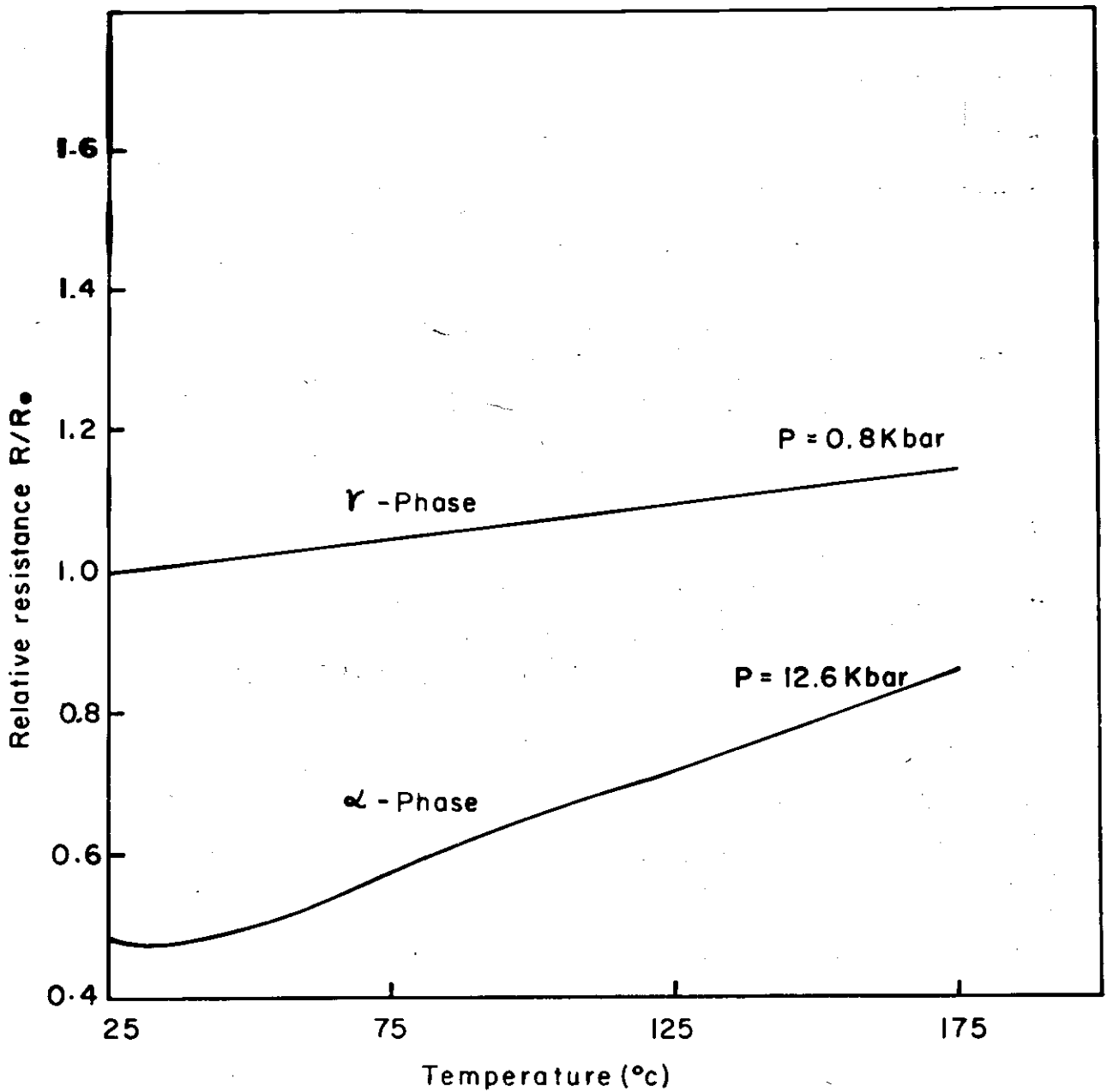


Fig.10. Relative resistance versus temperature graph.  $R_0$  is the resistance at 25 $^{\circ}\text{C}$  and 0.8 Kbar pressure.

Mean temperature = 275°C

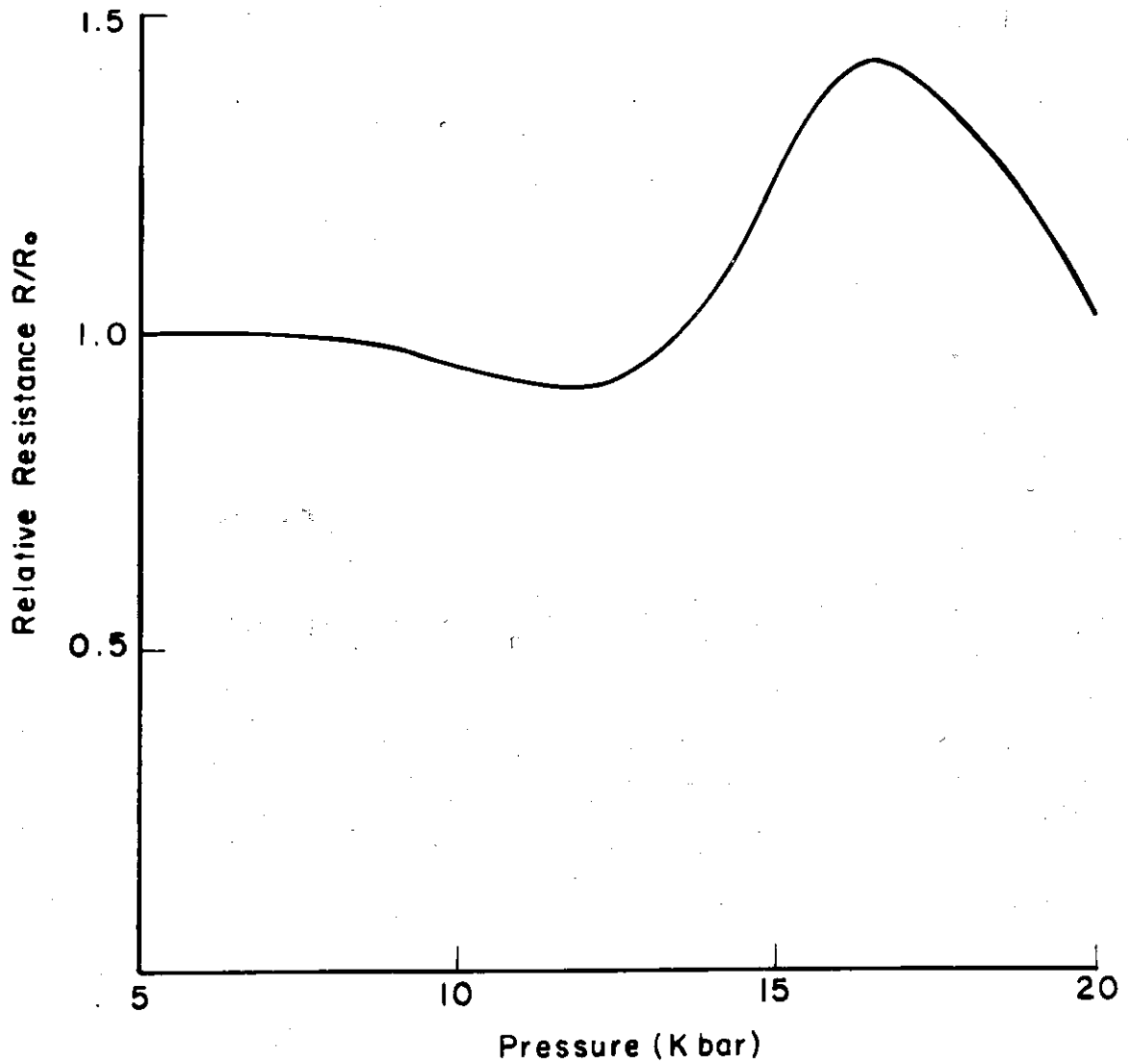


Fig. II. Relative resistance versus pressure graph above the critical point.  $R_0$  is the resistance at 275°C and atmospheric pressure.

and (iii) the resistivity continuously decreases at higher pressures. It is important to note that the features such as the resistivity minimum and the later rapid increase with pressure do not exist at a temperature below the critical point (see Figure 2).

## 6. Theoretical Discussion

### 6.1. Thermo-Electric Behaviour in the $\gamma$ -Phase:

The electron diffusion thermo-electric power is given, quite generally, by the expression (Mac Donald, 1962)

$$Q = - \frac{\pi^2 k^2 T}{3e} \left[ \frac{d \log n(E)}{dE} + \frac{d \log v^2(E)}{dE} + \frac{d \log \tau(E)}{dE} \right]_{E_F} \quad (1)$$

Here  $e$  is the magnitude of the elementary charge.  $\tau(E)$  and  $n(E)$  represent the relaxation time and the density of states respectively.  $v$  is an average electron velocity.

In this section an attempt will be made to explain the large pressure effect on the thermo-power of  $\gamma$ -Ce on the basis of the Friedel-Anderson model appropriate to cerium. According to the model developed for  $\gamma$ -Ce, the six-fold degenerate 4f level ( $J = \frac{5}{2}$ ) is split by the intra-atomic Coulomb interaction and exchange such that one of the sub-levels lies below and the other five are above the Fermi level. The effect of pressure is to reduce the separation between the lower occupied 4f sublevel and the Fermi level.

The thermo-power of  $\gamma$ -cerium, even at atmospheric pressure, is relatively large and positive of the order of  $+7 \mu\text{V}/^\circ\text{C}$  when compared with nearly  $-2 \mu\text{V}/^\circ\text{C}$  appropriate to the other rare earth metals (Born et al, 1961). This, we believe, is related to the proximity of the 4f state relative to the Fermi energy. The existence of a resonant state overlapping with the conduction band and lying just below the Fermi level has the effect of contributing an extra density of states at the Fermi level. This contribution is in addition to the regular band structure associated with the 6s - 5d band. Thus one could write for the total density of states at the Fermi level the expression

$$n(E_F) = n_0(E_F) + \rho(E_F) \quad (2)$$

Here  $n_0(E_F)$  represents the contribution from the 6s-5d band and  $\rho(E_F)$  is the extra factor due to the 4f virtual bound state below the Fermi energy.  $\rho(E)$  is given by the formula (Blandin et al, 1965)

$$\rho(E) = \frac{1}{\pi} \frac{\Delta}{(E - E_f)^2 + \Delta^2} \quad (3)$$

where  $\Delta$  is the width of the virtual level and  $E_f$  corresponds to the renormalized energy of the 4f state lying below the Fermi level. It is clear from equations (1) and (2) that the virtual 4f level makes a contribution to the thermo-power proportional to  $[\frac{d\rho(E)}{dE}]_{E_F}$  where

$$\left[ \frac{d\rho(E)}{dE} \right]_{E_F} = -\frac{2}{\pi} \frac{\Delta(E_F - E_f)}{[(E_F - E_f)^2 + \Delta^2]^2} \quad (4)$$

The contribution to the thermo-power due to the extra density of states factor at the Fermi level is given by

$$Q' = \frac{2\pi k^2 T}{3e} \frac{1}{n(E_F)} \frac{\Delta(E_F - E_f)}{[(E_F - E_f)^2 + \Delta^2]^2} \quad (5)$$

We note here that  $Q'$  is very sensitive to the position of the 4f state relative to the Fermi level and can even change sign. This can be seen more clearly by making an order of magnitude calculation for  $Q'$ . The level width  $\Delta$  is extremely small and is estimated from various studies (Huber and Maple, 1970) to be around 0.01 eV. Then for  $E_F - E_f \sim 0.2$  eV and  $n(E) \sim 2$  states/eV per atom, one gets  $Q' \sim +4$   $\mu\text{V}/^\circ\text{C}$ . When  $E_F - E_f \sim 0.1$  eV., the magnitude of  $Q'$  is large, of the order of  $+20$   $\mu\text{V}/^\circ\text{C}$ .

The thermo-power variation of  $\gamma$ -cerium with pressure (Figure 5) finds a simple explanation on the basis of the relation (5). In the entire  $\gamma$  phase region,  $(E_F - E_f)$  is positive so that  $Q'$  is positive and its magnitude becomes large with increasing pressure. If we assume that as far as the pressure variation is concerned, the major contribution to the thermo-power is from the  $Q'$  term, then one can understand the large increase in the magnitude of thermo-power

as the transition is approached. The contribution to the thermo-electric power from the regular band structure of the 6s-5d band can be either positive or negative depending on the energy dependence of the electron relaxation time and the normal density of states at the Fermi level. The term  $\left[\frac{d \log \tau(E)}{dE}\right]$  may be expected to make a significant contribution only when  $[E_F - E_f]$  is of the order of a few  $\Delta$ . In the absence of experimental data on the variation of  $[E_F - E_f]$  with pressure, it is not possible to make a quantitative prediction of the behaviour of the thermo-power. Further the relative importance of the different terms in equation (1) depends crucially on how close the 4f states approach the Fermi energy at high pressures.

## 6.2. The $\gamma$ - $\alpha$ Phase Transition:

The drastic decrease in the magnitude of the thermo-electric power accompanying the  $\gamma$ - $\alpha$  phase transition (Figure 5) may be attributed to the delocalization of the 4f electrons resulting in an enhancement of the conduction electron concentration. According to Thomson's point of view (Mac Donald, 1962), the thermo-electric power can be thought of, crudely, as the electronic specific heat per conduction electron. Although the electronic specific heat constant in the  $\alpha$  phase is large (Gschneidner, 1965) due to the enhanced density of

states at the Fermi level, this effect is masked by the additional contribution of nearly an electron per cerium atom to the conduction band. In other words, the increased magnitude of the Fermi energy in the  $\alpha$  phase relative to the  $\gamma$ -phase is responsible for the drop in the thermo-electric power.

### 6.3. Thermo-Electric Behaviour in the $\alpha$ -Phase:

The continuous decrease in the thermo-electric power of  $\alpha$ -Ce with pressure and the dramatic increase in the value of the thermo-power with temperature (Figures 5 and 8) can be correlated with the fractional valency model of  $\alpha$ -Cerium. Experimental evidence such as the Hall effect measurements (Gschneidner, 1964), magnetic susceptibility measurements at high pressures (Mac Pherson et al, 1971), absence of superconductivity in the  $\alpha$ -phase (Smith, 1965), etc. suggests that the 4f sublevels in  $\alpha$ -cerium, although they are located above the Fermi level, can still influence the different physical properties. According to the model developed for  $\alpha$  cerium, the 4f level is just above the Fermi level near 8 kbar pressure ( $\sim 0.05$  eV) and is shifted further from the Fermi level at higher pressures. Under these conditions, one should expect the temperature to have a significant effect on the transport properties.

In the Hirst's model for  $\alpha$  cerium (Hirst, 1970) the 4f virtual bound state gets 'locked up' with the Fermi level over a finite pressure region and such a thermodynamic state has unusual properties. For temperatures  $kT < \Delta$ , the system is in a well defined ionic configuration whereas at higher temperatures when  $kT \geq \Delta$ , the system should be described by a weighted average of the two configurations. It is important to recognize that the delocalization of 4f electrons should cause a dramatic increase in the Fermi energy. The different isotherms of the occupancy of the 4f states as a function of the parameter  $(E_f - E_F)$  given by Blandin et al (1965) shows that in the  $\alpha$ -phase, there is considerable excitation of the conduction electrons into the 4f states at high temperatures. In fact it is this feature which suggests the possibility of a first order transition terminating at a critical point.

The theoretical analysis of the thermo-power behaviour in the  $\alpha$ -phase is difficult because of the several factors involved in the problem. The anomalous temperature dependence of the thermo-power in the  $\alpha$ -phase (Figure 8) can be qualitatively understood on the basis that both the variation of the conduction electron density with temperature and the energy dependence of the relaxation time are important. The existence of a resonant state just above the Fermi level

causes the scattering cross-section of the conduction electrons to increase markedly with energy so that  $\left[\frac{d \tau(E)}{dE}\right]_{E_F}$  turns out to be negative. Thus the contribution of this term to the thermo-power is positive. Further the decrease in the conduction electron concentration with temperature due to partial excitation into 4f states results in an increase of the magnitude of the thermo-power. This is because the thermo-power is inversely related to the number density of mobile electrons. The electrons in the 4f state have much lower mobility and may be expected not to contribute directly to the electron diffusion process. The isobar at 20 kbar in Figure 8 shows that the rate of increase of thermo-power with temperature is much smaller than that at 10 kbar. This can be understood by noting that at higher pressures, the 4f state has moved sufficiently away from the Fermi level and the conduction electron density varies little with temperature. The energy dependence of the relaxation time would also be weaker when the resonant state lies significantly above the Fermi energy.

#### 6.4. Resistivity Behaviour in $\alpha$ and $\gamma$ Phases:

The strong temperature dependence of the resistivity in the  $\alpha$ -phase relative to the  $\gamma$  phase can be understood on the basis of the S or d - f scattering model. The nearly empty 4f level, characterized by a high density of states,

acts as a 'trap' for the current carrying 6s and 5d electrons. This is essentially the same mechanism as the Mott's s-d scattering model for the electronic properties of transition metals (Mott and Jones, 1936). In other words, the 4f level provides the alternative states for scattering when the separation ( $E_F - E_f$ ) is of the order of  $kT$ . If this model is right, then at low temperatures, viz.,  $kT \ll (E_F - E_f)$ , the rate of increase of resistivity with temperature in the  $\alpha$ -phase should be less marked than its behaviour at higher temperatures.

The resistivity behaviour above the critical point (Figure 11) finds a simple explanation. The shallow resistivity minimum observed near 12 kbar pressure may be attributed to the partial emptying of the 4f electrons (lying still below the Fermi level) into the conduction band. We may note here that  $kT \approx 0.05$  eV and the separation between the 4f state and the Fermi level near 12 kbar would be of the same order as  $kT$ . The increase in the resistivity between 12 to 17 kbar pressure is due to the 4f virtual bound state sweeping the Fermi surface. This behaviour will be absent in the first order phase transition (i.e., below the critical point) because of the abrupt shift in the position of the 4f level relative to the Fermi level. The magnitude of the resistivity rise is not too large because of the

rather large thermal spread near the Fermi level ( $\sim .05$  eV) compared with the much narrower level width of the 4f state ( $\sim .01$  eV). The fall in the resistivity near 18 kbar pressure is due to the delocalization of the 4f electrons, similar to the abrupt drop in the first order phase transition. The experimentally observed behaviour of the resistivity versus pressure above the critical point is in full accordance with the earlier prediction of Blandin et al (1965).

## 7. Conclusions

The thermo-electric power of cerium as a function of pressure has been studied over a wide temperature range which includes the region of both below and above the critical point. The resistivity data as a function of pressure above the critical point is also reported. A qualitative discussion of these experimental results on the basis of the Friedel-Anderson model has been presented.

**References**

- Alascio, B., Lopez, A. and Olmedo, C.F.E. (1973).  
J. Phys. F. : Metal Phys. 3, 1324.
- Anderson, P.W. (1961). Phys. Rev. 124, 41.
- Beecroft, R.I. and Swenson, C.A. (1960). J. Phys. Chem.  
Solids, 15, 234.
- Blandin, A., Coqblin, B. and Friedel, J. (1965).  
in Physics of Solids at High Pressures, ed. C.T. Tomizuka  
and R.M. Emrick (Academic Press, New York), P.233.
- Born, H.J., Legvold, S. and Spedding, F.H. (1961).  
J. Appl. Phys. 32, 2543.
- Bridgman, P.W. (1927). Proc. Am. Acad. Arts Sci. 62, 207.
- Coqblin, B. and Blandin, A. (1968). Advan. Phys. 17, 281.
- Franceschi, E. and Olcese, G.L. (1969). Phys. Rev. Lett.  
22, 1299.
- Friedel, J. (1954). Advan. Phys. 3, 446.
- Friedel, J. (1956). Can. J. Phys. 34, 1190.
- Gschneidner, K.A. and Smoluchowski, R. (1963).  
J. Less-Common Metals 5, 374.
- Gschneidner, K.A. (1964). Rare-Earth Research III,  
ed. L. Eyring, Gordon and Breach.
- Heeger, A.J. (1969) in Solid State Physics, Academic  
Press, New York, 23, p. 283.

- Hirst, L.L. (1970). *Phys. Kondens. Materie*, 11, 255.
- Huber, J.G. and Maple, M.B. (1970). *J. Low-Temp. Phys.*  
3, 537.
- Jayaraman, A. (1965). *Phys. Rev.* 137, A179.
- Kondo, J. (1969). in Solid State Physics, Academic Press,  
New York, 23, P.183.
- Landau, L.D. and Lifshitz, E.M. (1958). Statistical Physics,  
Pergamon Press, Ltd. P.260.
- Lawson, A.W. and Tang, T.Y. (1949). *Phys. Rev.* 76, 301.
- Mac Donald, D.K.G. (1962). Thermoelectricity, Wiley and  
Sons, New York, P. 12.
- Mac Pherson, M.R., Everett, G.E., Wohlleben, D. and Maple,  
N.B. (1971). *Phys. Rev. Lett.* 26, 20.
- Maines, R.G. (1970). *Rev. Sci. Instr.* 41, 1415.
- Maple, M.B. and Wohlleben, D. (1971). *Phys.Rev.Lett.* 27, 511.
- McWhan, D.B. (1970). *Phys. Rev.* B1, 2826.
- Mott, N.F. and Jones, H. (1936). Theory of the Properties  
of Metals and Alloys, Oxford.
- Ponyatovskii, E. (1958). *Soviet Physics, Doklady* 3, 498.
- Ramirez, R. and Falicov, L.M. (1971). *Phys. Rev.* B3, 2425.
- Ratto, C.F., Coqblin, B. and Galleani, D'Agliano, E. (1969).  
*Adv. Phys.* 18, 489.

Schuch, A.F. and Sturdivant, J.H. (1950). J.Chem.Phys.  
19, 145.

Smith, T.F. (1965). Phys. Rev. 137, A1435.

Wilkinson, M.K., Child, H.R., Mac Hargue, C.J., Koehler, W.C.  
and Wollan, E.D. (1961). Phys. Rev. 122, 1409.

Wittig, J. (1968). Phys. Rev. Lett. 21, 1250.

Wohlleben, D. (1968). Thesis, University of California.